ELSEVIER

Polymer 42 (2001) 6105–6112

polymer

www.elsevier.nl/locate/polymer

Solvent effects on aggregation behavior of polyvinyl alcohol solutions

Po-Da Hong*, Che-Min Chou, Chiu-Hui He

Department of Fiber and Polymer Engineering, National Taiwan University of Science and Technology, Taipei 10607, Taiwan ROC

Received 20 October 2000; received in revised form 22 December 2000; accepted 9 January 2001

Abstract

The present study elucidates the effects of solvent quality and polymer concentration on the aggregation behavior of polyvinyl alcohol (PVA) solutions from the dilute solution to semi-dilute solution regions. Combination of the results in static and dynamic light scattering indicates that in dilute solution the thermodynamic driving forces primarily dominate the dynamic behavior of PVA/*N*-methylpyrrolidone (PVA/NMP) solution. In contrast with PVA/water solution, the hydrodynamic interaction would dominate the dynamic behavior of the solution. The concentration dependence on the dynamic behavior of semi-dilute solution has also been studied through DLS measurement. For PVA/water solutions, the hydrodynamic correlation length of fast mode has a concentration dependence given by $\xi_D = [\eta]C^{-0.42}$, and the value of exponent is close to the predicted value from scaling theory in the marginal solvent. On the other hand, for PVA/NMP solutions the value of exponent is close to the predicted value from the scaling theory in good solvent limit: -0.75. However, contrary to the expectation, the gelation behavior could not occur in PVA/water solutions at the same condition of gelation in PVA/NMP solution even though the affinity of water to PVA is much lower than that of NMP. In this work, we considered that the PVA/NMP solution might possess a character that could form a homogeneous network structure. The intermolecular associations must play a dominant role as soon as the chains start to overlap in PVA/NMP solution. On the other hand, combining the DLS result with our previous work, the gelation of PVA/NMP solutions is considered due to complex formation in the transient network junctions, i.e. the formation of molecular complex is crucial to the physical gelation in a good solvent system.

Keywords: Polyvinyl alcohol; Solvent effects; Aggregation behaviors

1. Introduction

Physical polymer gel is a three-dimensional network of polymer chains cross-linked by physical association. It is well known that many factors affect the gelation behavior of the polymer solution, such as the temperature, concentration of polymer, and the type of solvent used. In our previous paper [1], we confirmed that the effects of the phase separation and crystallization on gelation of polyvinylidene fluoride/tetra (ethylene glycol) dimethyl ether solutions in terms of thermodynamic and kinetic aspects, and at the onset elucidated that the gelation in phase separation system could be divided into two regions by a kinetic transition concentration, $C^*_{tran.}$. On the other hand, we also explain the characteristics of PVC solutions at various concentration regions and their influence on the structural formation of gels with spinodal decomposition process [2]. Moreover, in order to understand the nature of gelation in phase separation system, we have studied the aggregation behavior of polyvinyl chloride/dioxane solution [3], and pointed out that the polymer–solvent interaction plays an important role in the dynamic and aggregation behaviors of polymer chains in solution states. The dynamic light scattering (DLS) results indicate that the dynamic behavior of PVC solution could be classified into three regions by increasing the concentration of PVC. The poor affinity of the solvent used should favor the intramolecular aggregation of polymer chains, resulting in comparatively complex dynamic behaviors in semi-dilute solutions.

Polyvinyl alcohol (PVA) is well known as a crystalline polymer, and it has been generally suggested that the gelation originates from phase separation and crystallization in the semi-dilute solutions prepared from various solvents [4–9]. In the previous papers [4,5], we have studied the structure and properties of PVA gels from *N*-methylpyrrolidone (NMP) solutions, and pointed out that the transparent PVA/NMP gels have a homogeneous and stable network structure. Meanwhile, the gelation could not occur in PVA/water solution at the same experimental conditions even though the attractive interaction between PVA and water is much lower than that between PVA and NMP. Experiments for semi-dilute solutions with various degrees

* Corresponding author. Tel.: +886-2-27376539; fax: +886-2-27376544.

E-mail address: phong@hp730.tx.ntust.edu.tw (P.-D. Hong).

0032-3861/01/$ - see front matter
PII: S0032-3861(01)00056-8

of solvent quality, such as θ, good, and marginal solvents, have been reported by many groups [10–20]. It is doubtless that the solvent quality must dominate the chain aggregation in the solution state.

In this work, the relation between the chain aggregation and the polymer–solvent interaction for PVA solutions from the very dilute into the semi-dilute regimes was first studied through the dynamic light scattering experiments. Then effects of solvent quality on the mechanism of chain aggregation were investigated to explain the gelation behavior of PVA solution in good solvent system.

2. Experimental section

2.1. Materials

A PVA powder ($\bar{M}_w = 155,000$, $\bar{M}_w/\bar{M}_n = 1.95$, Aldrich Chemical Co. Ltd, USA) with a high degree of hydrolysis (about 99 + %) was used in this work. The distilled water and analytical grade solvent NMP were repeatedly filtered using a 0.02 μm Teflon filter for removing dust. The PVA solutions were prepared in a precleaned wide mouth bottle, with stirring at 95°C for 2 h until they dissolved into homogeneous solutions. The PVA solutions with the concentration of 0.1–1 g dl^{-1}, were filtered using a 0.45 μm Teflon filter, then cooled into a thermostat oven at constant temperature 30°C for one day to stabilize the solutions before the measurements.

2.2. Dynamic light scattering

The measurements were performed on a Malvern series 4700 apparatus, in combination with a 2 W argon ion laser operating at a power of 100 mW and a wavelength of 514 nm. The measurement was carried out with the 7132 multiple-τ autocorrelator recording on 128-channels. All data, as obtained in the intensity autocorrelation function, were measured at the scattering angle, θ in the range of 30–120°. DLS is a highly effective tool for probing the dynamic behavior of polymer chains, on different length and time scales, in solution states. When the polymer chain obeys Gaussian statistics, the measured normalized intensity correlation function $g^{(2)}(t)$ is related to the normalized electric correlation function $g^{(1)}(t)$ through the Siegert relation [21]:

$$g^{(2)}(t) = 1 + \beta|g^{(1)}(t)|^2 \tag{1}$$

where β takes into account the deviations from the ideal correlation. Consider a system exhibiting a distribution of collective motions, which can be represented by a superposition of exponential decays, and allowing the monitoring of very widely spaced decays in the same investigation. Laplace inversion routine of the correlation curves $g^{(1)}(t)$ was performed using a CONTIN [22] to obtain the distribution $A(\tau)$ of relaxation times. The Laplace inversion routine was given as follows:

$$g^{(1)}(t) = \int_0^\infty A(\tau)\exp(-t/\tau)\,\mathrm{d}\tau \tag{2}$$

2.3. Viscosity

The intrinsic viscosity measurements were made on dilute PVA solution at 30 ± 0.1°C using an Ubbelohde capillary viscometer. The intrinsic viscosity, $[\eta]$ was obtained using the Huggins equation [23]:

$$\frac{(t-t_0)/t_0}{C} = \frac{\eta_{sp}}{C} = [\eta] + k'[\eta]^2 C \tag{3}$$

where t is the time of flow of the dilute solution, t_0 the time of flow of the pure solvent, C the concentration of polymer, η_{sp} specific viscosity and k' is the Huggins constant. The viscosity of PVA semi-dilute solution was measured using a CJV1000 vibroviscometer [24] (Tohoku Densi Co. Ltd, Japan). PVA solutions were heated at 95°C until they dissolved into a homogeneous solution, and then were quickly cooled to 30°C.

3. Results

3.1. Dilute solution

Recently, in our previous study [25], we reported the results from the Zimm plots of PVA solutions, and manifested that the values of second virial coefficient, A_2, for PVA/NMP and PVA/water solutions are 23.3×10^{-4} and 1.8×10^{-4} ml mol g^{-2} at 30°C, respectively. This result illustrates that the interaction between PVA and water is much lower than that between PVA and NMP. Moreover, it may be considered that the water is marginal solvent for PVA molecules, i.e. there are only weak excluded-volume interactions and the PVA chains are nearly ideal on all length scales [10,42]. The results inferred form the Zimm plot also showed that the R_g value (ca. 47.8 nm) for PVA/NMP solution is much larger than that (ca. 21.3 nm) for PVA/water solution.

Fig. 1 shows the reduced viscosity, η_{sp}/C, as a function of the PVA concentration, C, consequently obtaining $k' = 0.23$ and $[\eta] = 2.40$ dl g^{-1} in PVA/NMP solution and $k' = 0.53$ and $[\eta] = 1.01$ dl g^{-1} in PVA/water solution. It is well known that the value of the Huggins constant, k', could also be used to predict the degree of the polymer–solvent interaction. In θ solvent ($k' = 0.52$), the polymer chains exhibit unperturbed coils. In a good solvent ($k' < 0.52$), the polymer chains should exhibit relatively extended conformations, and in a poor solvent ($0.8 < k' < 1.3$), the polymer chains collapse and the intramolecular aggregation occurs easily. Therefore, the final interpretations simultaneously manifest that NMP is a good solvent ($k' = 0.23$; $A_2 = 23.3 \times 10^{-4}$ ml mol g^{-2}) for PVA but water is quite close to a θ solvent ($k' = 0.53$; $A_2 = 1.8 \times 10^{-4}$ ml mol g^{-2}) for

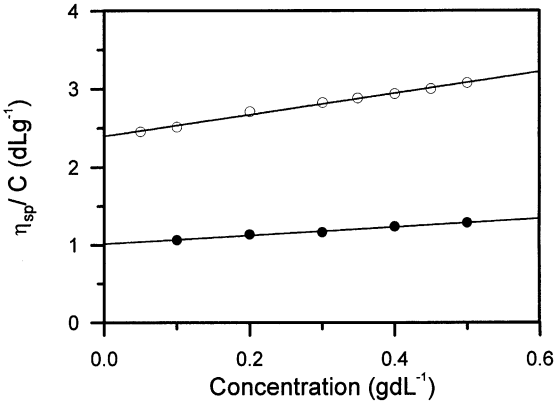

Fig. 1. The reduced viscosity, η_{sp}/C, as a function of C at 30°C.

PVA at 30°C. The interaction between PVA and NMP (or water) could be comprehended by the donor–acceptor electron properties. NMP, a typical dipolar aprotic solvent, could either be a strong electron donor or a hydrogen acceptor to enhance the affinity between PVA and NMP. The double bond between the oxygens of NMP could form more stable H-bonding with the hydroxyl groups of PVA, and broke the H-bonding within the PVA hydroxyl groups; therefore the 'C=O' group of NMP is a 'strong site' for PVA. On the other hand, the 'O–H' group of water is only a 'weak site' for PVA which just products weak H-bonding between PVA and water. On the other hand, the chain overlapping concentration C^* is frequently defined by the reciprocal of the intrinsic viscosity, $1/[\eta]$. The C^* values are about 0.42 g dl^{-1} for PVA/NMP solution, and 0.99 g dl^{-1} for PVA/water solution, respectively.

Fig. 2(a) and (b) shows, respectively, the intensity time correlation functions, $g^{(2)}(t) - 1$, for the PVA/water and PVA/NMP solutions at 30°C together with the corresponding relaxation time distributions obtained by using the inversion Laplace transformation. The distribution of the $\tau A(\tau)$ results indicated that the PVA dilute solutions, in which the concentration is below the C^*, exhibited a single relaxation mode, and the decay rate, $\Gamma = 1/\tau$ (inset of Fig. 2), for both the relaxation modes showed a linear dependence with the square of the scattering vector, q^2. These single modes are attributed to the translational diffusion of individual PVA coil in solutions. When $qR_g \ll 1$, the mutual diffusion coefficient is defined as $D = \Gamma/q^2$. The values of the mutual diffusion coefficient of PVA as a function of concentration for PVA/water and PVA/NMP solutions at 30°C are shown in Fig. 3. Clearly, at a given temperature the mutual diffusion coefficient varies with the polymer concentration and solvent quality.

Generally, the mutual diffusion coefficient at a finite concentration can be characterized by the concentration coefficient, k_D, as follows [26–28]

$$D = D_0(1 + k_D C + \cdots) \quad (4)$$

where D_0 is the mutual diffusion coefficient at infinite

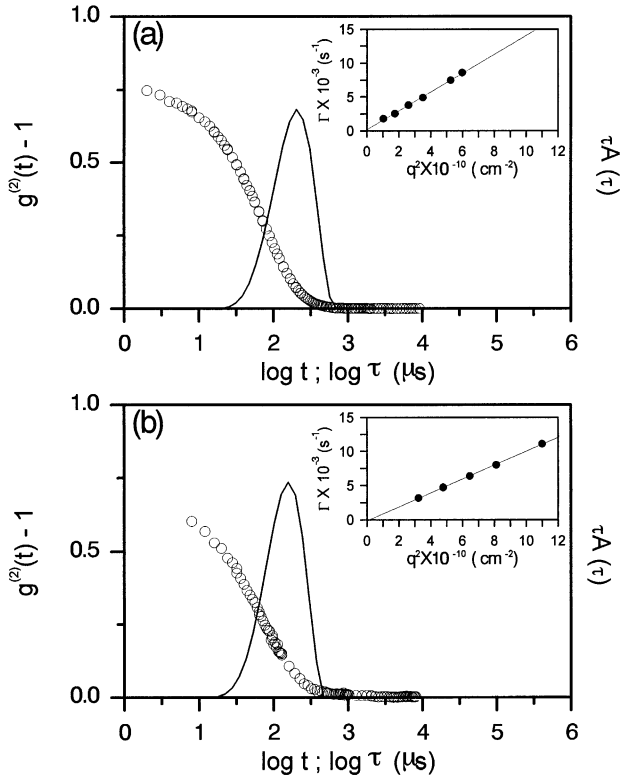

Fig. 2. The normalized intensity–intensity autocorrelation function, $g^{(2)}(t) - 1$, for dilute solutions of PVA in: (a) water (0.56 g dl^{-1}; $[\eta]C = 0.56$); and (b) NMP (0.2 g dl^{-1}; $[\eta]C = 0.48$) at 30°C and a scattering angle $\theta = 90°$, along with their corresponding distributions of relaxation times, obtain by using the inversion Laplace transformation. Inset: q^2 dependence of the corresponding decay rate, Γ.

dilution, D the value of concentration function, and k_D is the second virial coefficient of the diffusion coefficient. In this expression the k_D can be separated into two parts: the first contribution is from the thermodynamic interaction, which is involved the second virial coefficient, A_2; and the second contribution is related to the hydrodynamic friction, which is involved the linear term in the concentration expansion for the friction coefficient, k_s. These parameters incorporated in k_D^{φ} are related according to: $k_D^{\varphi} = 8X^3 - k_s^{\varphi}$,

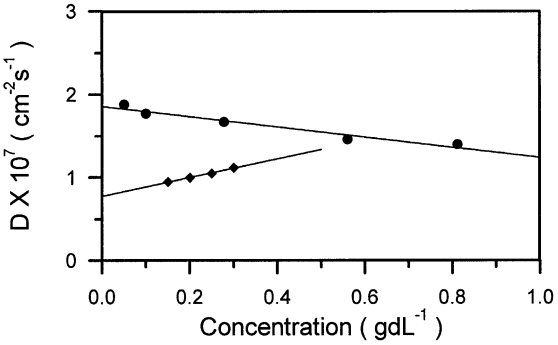

Fig. 3. The diffusion coefficient D as a function of PVA concentration at 30°C: (●) PVA/water; (◆) PVA/NMP.

Table 1
Characteristic parameters of diluted PVA solution in various solvents at 30°C

	A_2 ($\times 10^{-4}$ ml mol g^{-2})	k_D (dl g^{-1})	k_D^{ϕ}	$8X^3$	k_s^{ϕ}	R_g (nm)	R_h (nm)
PVA/water	1.8	−0.33	−0.6	1.15	1.75	21	15
PVA/NMP	23.3	1.45	1.72	8.83	7.13	48	17

where the superscript is expressed in volume fraction unit, and $X \equiv \bar{S}/R_h$ and $\bar{S}$ is a fictive radius of the equivalent thermodynamic sphere which is defined in terms of the second virial coefficient by $\bar{S} = (3M^2A_2/16\pi N_A)^{1/3}$. On the other hand, the hydrodynamic radius R_h can be also evaluated from the diffusion coefficient at infinite dilution, D_0, using Stokes–Einstein relation: $R_h = k_B T/6\pi\eta_0 D_0$, where k_B is the Boltzmann constant, and η_0 is the solvent viscosity. These calculated parameters are summarized and shown in Table 1. From Fig. 3 and Table 1, in the good solvent region k_D takes a positive value and the diffusion coefficient increases with the concentration. It may be concluded that the thermodynamic driving forces primarily dominate the dynamic behavior of dilute PVA/NMP solution. In contrast to that of the PVA/water solution, the negative value of k_D is in agreement with the theoretical calculation that predicts a nonzero negative value near the θ region, indicating that the hydrodynamic interaction would dominate the dynamic behavior of PVA/water solutions.

3.2. Semi-dilute solution

In a dilute solution, it is well known that the dynamic behavior of the polymer coil is highly sensitive to the solvent quality. At high concentrations the effects of chain entanglements become more important and the solvent effect on polymer aggregation may be weakened. However, the effects of solvent and concentration on chain aggregation are reflected primarily at the semi-dilute concentration region and have been demonstrated by a scaling theory [10]. The present study primarily explains the dynamic characteristics of PVA solutions at the various concentration regions and the influence of the solvent used on the aggregation behaviors. The concentration dependence on the dynamic behavior of polymer solutions has been extensively studied through DLS measurements. Owing to the various mechanisms of chain aggregation in polymer solutions, the origin of the relaxation modes in DLS results become very complex [29–36]. Herein, we try to investigate the effect of the polymer–solvent interaction on the aggregation behavior of PVA chains from dilute to semi-dilute solution regions through DLS analyses.

Generally, the chain aggregation in polymer solutions should take place beyond the chain overlapping concentration. Frisch and Simha [37] reported that the dynamic behavior of the polymer solution could be classified into several regions using the semi-empirical rules according to the interaction degree of the polymer with its environment. According to their classification the dynamic behavior of the polymer solution is usually separated into four different concentration regions, i.e. the infinite dilution limit; hydrodynamic screening limit; polymer–polymer contact region; and polymer chain entanglement region. In the infinite dilution limit, defined as a concentration below $[\eta]C \sim 1$, the polymer chain acts as an isolated coil. If the concentration of the polymer in the solution is raised, the hydrodynamic screening limit will be reached when the relative proximity of the neighboring chains allow polymer–polymer intermolecular interactions to influence the motion of the polymer chains. Perturbation of the polymer motion by this mechanism is expected to occur above a concentration defined by $[\eta]C > 1$. The effects may be expected to be cumulative up to concentrations corresponding to the chain overlapping concentration, which is the close packing of polymer coils in solution, $[\eta]C \sim 4$. Once the overlapping concentration has been reached, the polymer motion will be dominated by the presence of direct polymer–polymer interactions. If the increasing concentration rises above the limit $[\eta]C \sim 10$, the interpenetration of the polymer coils or the pseudo-matrix-gel will be formed. To obtain more detailed information on the characteristics of the PVA solution over a wide concentration region, including both dilute and semi-dilute solutions, generally the product $[\eta]C$ is made equivalent to the reduced concentration, and can be employed as a simple, approximate, overlap criterion for the dynamic behavior of polymer solution.

3.3. PVA/water solution

Fig. 4 illustrates typical intensity time correlation functions,

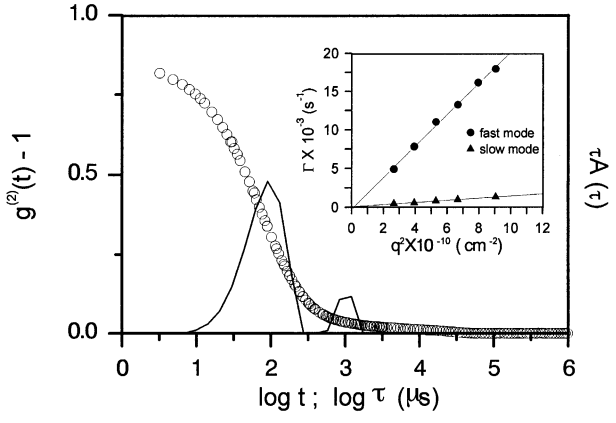

Fig. 4. The normalized intensity–intensity autocorrelation function, $g^{(2)}(t) - 1$, for semi-dilute PVA/water solutions (6 g dl^{-1}; $[\eta]C = 6.1$) at 30°C and $\theta = 90°$, along with the corresponding distributions of relaxation time. Inset: q^2 dependence of the corresponding two decay rates, fast (●) and slow (▲).

$g^{(2)}(t) - 1$, measured at semi-dilute concentration, $[\eta]C = 6.1$, together with the corresponding relaxation time distributions obtained by using the inversion Laplace transformation. Distinct change in the shape of the correlation function is found with an increasing concentration beyond $[\eta]C = 1$. Two relaxation modes denoted as the fast and slow modes from the $\tau A(\tau)$ distribution at short τ to the long τ in order were observed. This result indicates that the chain aggregation behavior is dependent much on the polymer concentration for PVA/water semi-dilute solutions. The decay rate, $\Gamma = 1/\tau$ (inset of Fig. 4), for both the relaxation modes are formally diffusive shown as a linear dependence with the square of the scattering vector. To obtain more detailed information on the characteristics of the PVA/water solution over a wide concentration region, Fig. 5 shows the value of relaxation rate for each relaxation mode as a function of the $[\eta]C$ value. At a concentration below $[\eta]C \sim 1$ in the infinite dilution region, Γ slightly decreases with the increasing concentration, indicating that the hydrodynamic interaction would dominate the dynamic behavior of PVA/water solutions. Then the two major relaxation modes are first observed in the hydrodynamic screening region, $1 < [\eta]C < 4$. In this region, the polymer–polymer intermolecular interaction will begin to influence the dynamic behavior of the polymer chains in solution.

First, Γ for the slow mode observed in the hydrodynamic screening region decreases slightly with an increasing concentration of the polymer. This fact can be attributed to either the dust or the cluster formed from the aggregation of several individual coils. A similar phenomenon has been obtained by numerous DLS experiments on semi-dilute systems [38–41]. At a concentration beyond $[\eta]C \sim 4$, the concentration region corresponds to a condition where the polymer coils begin to overlap, the intermolecular aggregation behavior becomes more conspicuous. The relaxation rate of the slow mode decreases rapidly as the concentration is further increased. It may be considered to be because of the heterogeneous transient gel network originated from the aggregation of the clusters in the concentrated PVA/water solutions.

It is interesting that there is a dramatic change in the slope at $[\eta]C \sim 4$ for the fast mode in Fig. 5. When $q\xi \ll 1 \ll qR_g$, the cooperative diffusion coefficient, D_c, is obtained as [42]

$$D_c = \frac{\Gamma}{(1-\phi)q^2} \tag{5}$$

where $(1-\phi)$ is the solvent backflow, and ϕ is the polymer volume fraction. Moreover, the hydrodynamic correlation length, ξ_D, can be evaluated from the relationship: $\xi_D = kT/6\pi\eta_0 D_c$ for each concentration as also shown in Fig. 5. At a concentration beyond the coil–coil interpenetrations, the hydrodynamic correlation length of the fast mode has a concentration dependence given by $\xi_D \sim [\eta]C^{-0.42}$. This value of the exponent is close to the predicted value from scaling theory in the marginal solvent: -0.5 [10,42] and a similar value has been obtained in the earlier reports on polystyrene in marginal solvents [38,43].

3.4. PVA/NMP solution

Figs. 6 and 7 show the time correlation functions, $g^{(2)}(t) - 1$, measured at semi-dilute concentrations, $[\eta]C = 2.4$ and $[\eta]C = 7.2$, respectively, together with the corresponding relaxation time distributions obtained by using the inversion Laplace transformation. It is very interesting that the distribution of the $\tau A(\tau)$ results for the PVA/NMP solutions in the hydrodynamic screening region still exhibit two relaxation modes, and both the decay rates, Γ, showed linear dependencies with q^2. On the other hand, three relaxation modes denoted as fast, middle and slow modes in Fig. 7 were found at the concentration region where the polymer coils begin to overlap. Generally, when the viscoelastic

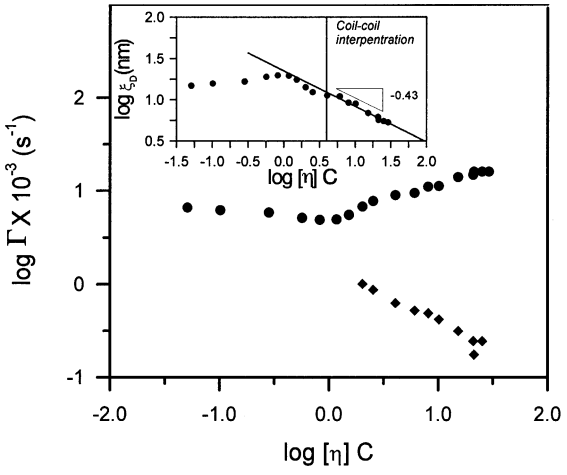

Fig. 5. log–log plots of the relaxation rate, Γ, versus $[\eta]C$ for PVA/water solutions at 30°C and $\theta = 90°$: (●) fast mode; and (◆) slow mode. Inset: concentration dependence of the hydrodynamic correlation length of the fast mode for semi-dilute PVA/water solutions.

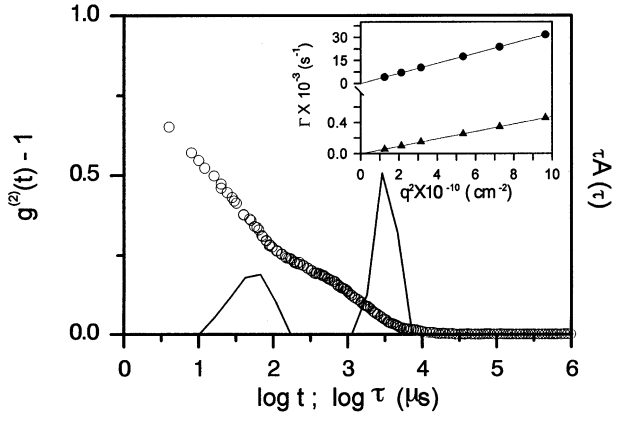

Fig. 6. The normalized intensity–intensity autocorrelation function, $g^{(2)}(\tau) - 1$, for semi-dilute PVA/NMP solution (1 g dl^{-1}; $[\eta]C = 2.4$) at 30°C and $\theta = 90°$, along with the corresponding distributions of relaxation time. Inset: q^2 dependence of the corresponding two decay rates, fast (●) and slow (▲).

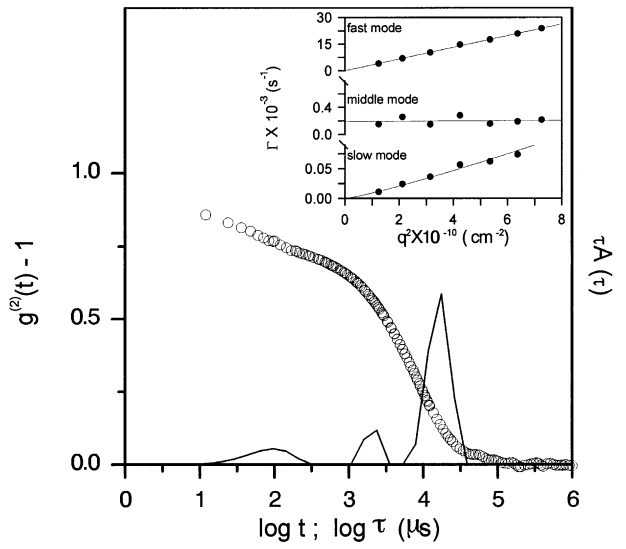

Fig. 7. The normalized intensity–intensity autocorrelation function, $g^{(2)}(\tau) - 1$, for semi-dilute PVA/NMP solutions (3 g dl^{-1}; $[\eta]C = 7.2$) at 30°C and $\theta = 90°$, along with the corresponding distributions of relaxation time. Inset: q^2 dependence of the corresponding two decay rates.

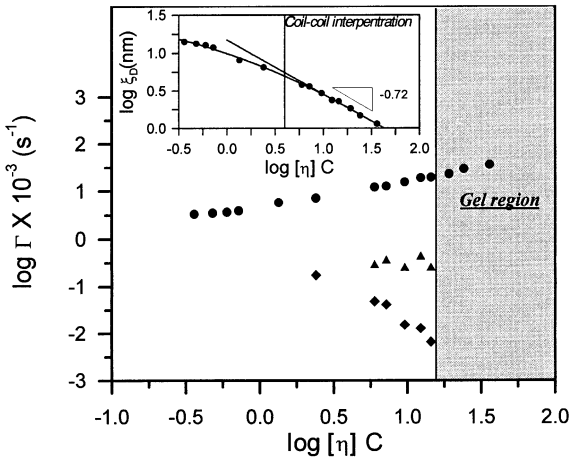

Fig. 8. log–log plots of the relaxation rate, Γ, versus $[\eta]C$ for PVA/NMP solutions at 30°C and $\theta = 90°$: (●) fast mode; (▲) middle mode; and (◆) slow mode. Inset: concentration dependence of the hydrodynamic correlation length of the fast mode in semi-dilute PVA/water solutions.

effect of the pseudogel is negligible the observed correlogram in a good solvent system is found to be consistent with a single-exponential decay, and the relaxation mode should relate to the hydrodynamic correlation length [44,45]. However, in the present study, the complexity of the relaxation time distribution was found in PVA/NMP semi-dilute solutions. In Fig. 7, the relaxation time of the major peak is plotted as a function of q^2. It is clear that both the fast and slow modes are diffusive but the middle mode is essentially independent of the scattering vector. Brown et al. [39,41] suggested that the q-independent mode might be related to the disentanglement time; in other words, it derives from a structural relaxation characterizing the lifetime of transient gels. According to this viewpoint, we may postulate that the middle mode is related to the viscoelastic properties of the transient network. However, our present study does not have enough evidence to infer the source of this mode.

Fig. 8 shows the individual decay rate, Γ, as a function of the $[\eta]C$ for PVA/NMP solutions at 30°C in a log–log diagram. As stated above, there are two or three relaxation modes at the semi-dilute region. The two major relaxation modes (fast and slow) are observed in the concentration region close to $[\eta]C \sim 2$, and three relaxation modes denoted as fast, middle and slow modes appeared at a concentration beyond $[\eta]C \sim 4$. Owing to the fact that the fast mode is diffusive, the hydrodynamic correlation length can be evaluated for each concentration as shown in Fig. 8. At the concentration beyond $[\eta]C \sim 4$, the hydrodynamic correlation length of the fast mode has a concentration dependence given by $\xi \sim [\eta]C^{-0.72}$. This value of the exponent is very close to the predicted value from the scaling theory in the good solvent limit: -0.75 [10,44,45]. On the other hand, the relaxation rate of the slow mode exhibits a negative dependence on concentration. Although NMP is a thermodynamically good solvent for PVA, from the q^2 dependence of its relaxation rate, it may also imply that the slow mode is related to the translational diffusion of clusters. Brown et al. [39,41,46] has also reported a similar phenomenon in semi-dilute solutions, and then concluded the cluster formation to be a source of slow mode representing the precursor stage in network formation.

It is interesting that the gelation occurs in the concentration beyond $[\eta]C \sim 12$ at our experimental conditions for PVA/NMP solution and the gel exhibits only a single relaxation mode, which corresponds to the fast cooperative mode in the PVA semi-dilute solutions. This phenomenon has also been found for the gel prepared from chemically cross-linked PVA aqueous solution using glutaraldehyde [46]. On the other hand, one might expect that the slow mode would be vanished because of the gel formation by the aggregation of clusters or the transient networks associate and the middle mode corresponding to a structural relaxation process would be restricted by a process of physical cross-linking. Under these considerations, we may suggest that the PVA/NMP gels should exhibit a character of homogeneous network structure.

4. Discussion

The relation between the dynamic behavior and the properties of polymer solutions is commonly investigated in terms of the viscometric study. As the polymer concentration is increased, the viscosity is mainly governed by the degree of the intermolecular interaction, which is usually connected with the overlapping of polymer chains [52–56]. Fig. 9 shows the log–log plot of η_{sp} versus $[\eta]C$ of PVA solutions, in which η_{sp} is defined by $\eta_{sp} = \eta/\eta_0 - 1$, η and η_0 are the viscosity of polymer solution and pure solvent,

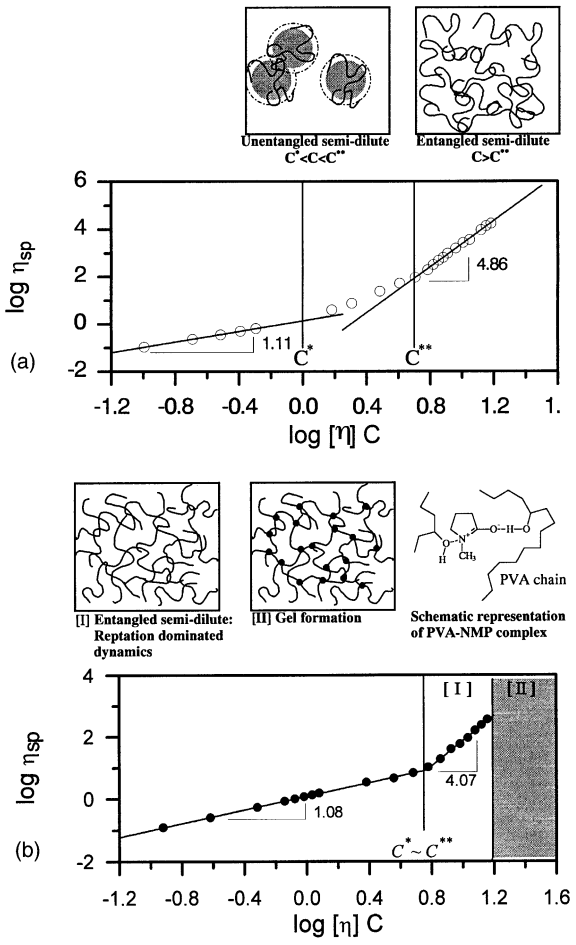

Fig. 9. The log–log plots of η_{sp} versus $[\eta]C$and the corresponding models of chain aggregation: (a) PVA/water; (b) PVA/NMP solutions.

respectively. Two asymptotic lines can fit the data and the exponential values are obtained from the slope of each concentration region are 1.08 and 4.07 for PVA/NMP solution, and 1.11 and 4.86 for PVA/water solution, respectively.

According to the characteristics of viscoselastic behavior and the semi-empirical rules proposed by Frisch and Simha, the relationship between the viscosity and reduced concentration could be divided into two or three distinguishing regions. In Fig. 9(a), the viscosity of the PVA/water solution has no significant change with concentration below the $[\eta]C < 1$ region. In this region, the polymer is sufficiently isolated and the other chains could not perturb the flowing behavior on polymer chains, and then the exponential value '1' represents a common behavior of dilute solution, which can be expressed by Huggins equation. Subsequently, the viscosity increases slightly at the concentrations between ca. $[\eta]C \sim 1$ and $[\eta]C \sim 4$. As mentioned earlier, the polymer–polymer intermolecular interaction will be allowed to influence the polymer motion in this region. These interactions can be considered to be of two types, i.e. the relatively close proximity of neighboring chains described by the hydrodynamic screening interaction and the collision of the chain coils for the cluster formation. The relatively poor affinity of water to PVA chains must increase the hydrodynamic friction, resulting in the increase in the viscosity of polymer solution. This fact could also be confirmed by DLS results.

As the concentration is further increased more than the chain overlapping concentration, $[\eta]C \sim 4$, the viscosity increases markedly, indicating that the polymer chains entangle with each other. The viscosity follows a power law of the reduced concentration with an exponential value close to a theoretical value '5' predicted by Adam et al. [56]. Experimentally rather used $C^*$and C^{**} to distinguish these concentrations regimes: (1) the dilute regime $C < C^*$ ($[\eta]C < 1$); (2) the hydrodynamic screening or the semi-dilute unentangled regime $C^* < C < C^{**}$ ($1 < [\eta]C < 4$); and (3) the semi-dilute entangled regime $C > C^{**}$ ($[\eta]C > 4$) where the polymer coils are strongly overlapped.

Fig. 9(b) shows the viscometric result for PVA/NMP solution and the viscosity rises very steeply beyond a critical concentration $[\eta]C > 5$. The viscosity property could be described by the reptation model in good solvent for semi-dilute solution following a power law of the reduced concentration with an exponential value close to a theoretical value '4' [56]. However, the crossover between the two viscosity regimes is well defined and much sharper than that of PVA/water solution. At the intersection point of two asymptotic lines, the infinite dilution limit C^* was considered identically to be the chain overlap threshold concentration or the concentration at the semi-dilute entangled regime. Thus, the results of Fig. 9(b) suggest clearly that the intermolecular associations play a dominant role as soon as the chains start to overlap for PVA/NMP solution.

The results as mentioned above indicate that the formation of PVA/NMP gel with a homogeneous network structure takes place in the concentration region beyond $[\eta]C \sim 12$. A similar behavior has been reported by Brown et al. [46] who compared the dynamic correlation length in PVA solutions and permanent gels prepared by chemical cross-linking using glutaraldehyde. Their results pointed out that the dynamic behavior of PVA gels would be essentially unaffected by the presence of the sparse cross-links. Then the relationship between the dynamic correlation length and the concentration in the permanent gels gives a value of exponent in accordance with scaling prediction for semi-dilute solutions. The dynamic correlation length for this permanent gel is almost twice that for the corresponding solution. However, it does not resemble the system in the gels formed by physical association such as PVA/NMP gels in this work. In the present case, the dynamic correlation length evaluated respectively from the PVA/NMP gel and solution is almost the same, as shown in Fig. 8. This discrepancy may be considered due to the average distance between the spatial neighbor junction points, which are enlarged by a bridging mechanism

with a fixed length and larger size of the glutaraldehyde molecule. The assumption that is generally made is that the physical gels differ from the chemically cross-linked gels because of the diversity of the essence at the junction point.

Our earlier studies [4,5] have indicated that the X-ray diffraction result in the PVA/NMP gels only showed a broad amorphous scattering peak even though PVA is well known as a crystalline polymer. Hence, we may consider that the gelation of PVA/NMP solutions was not induced by crystallization to form homogeneous and transparent gels. NMP is a typical dipolar aprotic solvent, because of the doubly bound oxygen is a strong electron donor or, in other words, a good hydrogen acceptor [47–49]. On the other hand, King et al. [50] and Guven et al. [51] have discussed the aggregation behavior in semi-dilute poly(*N*-vinyl-2-pyrrolidone)/water system which the molecular interaction is similar to this work. Although the functional groups of the polymer and solvent are just the reverse of this work. Their results strongly suggested a mechanism for the complex formation between poly(*N*-vinyl-2-pyrrolidone) and water molecules. In other words, the tetrahedral hydrogen bond network of water could effectively link the polymer chains together. On the other hand, we recently reported [25] that one NMP molecule could bind with two water molecules to form NMP(water)$_2$ ter-solvency complex in PVA/NMP/water solution. According to the reasoning from analogy among these solution systems, we may consider that the gelation of PVA/NMP solutions is induced by the formation of polymer–solvent complexes, which act the junction points in the transient gel network. The mechanism of polymer–solvent complex in PVA/NMP solutions is also schematically illustrated in Fig. 9(b). As compared with the physical gelation through phase separation or crystallization in other poor solvent systems, the formation of the polymer–solvent complex must be crucial for gelation in a good solvent system.

Acknowledgements

The authors wish to thank the National Science Council of the Republic of China for financial aid through project NSC88-2216-E011-026.

References

[1] Hong PD, Chou CM. Polymer 2000;41:8311.
[2] Hong PD, Chou CM. Macromolecules 2000;33:9673.
[3] Hong PD, Chou CM, Chen JH. Polymer 2000;41:5847.
[4] Hong PD, Miyasaka K. Polymer 1991;32:3140.
[5] Hong PD, Chen JH, Wu HL. J Appl Polym Sci 1998;69:2477.
[6] Genent J. Thermoreversible gelation of polymers and biopolymers. London: Academic Press, 1992.
[7] Oukura M, Kanaya T, Kaji K. Polymer 1992;33:3869.
[8] Oukura M, Kanaya T, Kaji K. Polymer 1992;33:5044.
[9] Hosea TJC, Ng SC. Polymer 1986;27:1804.
[10] de Gennes PG. Scaling concepts in polymer physics. London: Cornell University Press, 1979.
[11] de Gennes PG. Macromolecules 1976;9:587.
[12] de Gennes PG. Macromolecules 1976;9:594.
[13] Daoud M, Cotton JP, Farnoux B, Jannink G, Sarma G, Benoit H, Duplessix R, Picot C, de Gennes PG. Macromolecules 1975;8:804.
[14] Adam M, Delsanti M. Macromolecules 1985;18:1760.
[15] Amis EJ, Han CC, Matsushita Y. Polymer 1984;25:650.
[16] Takahai M, Nose T. Polymer 1986;27:1071.
[17] Nicolai T, Brown W, Johnsen RM, Stepanek P. Macromolecules 1990;23:1165.
[18] Nicolai T, Brown W, Hvidt S, Heller K. Macromolecules 1990;23:5088.
[19] Wang CH. Macromolecules 1992;25:1524.
[20] Sun Z, Wang CH. Macromolecules 1996;29:2011.
[21] Chu B. Laser light scattering. 2nd ed. San Diego, CA: Academic Press, 1991.
[22] Provencher SW. Comput Phys Comm 1982;27:213.
[23] Spering LH. Introduction to physical polymer science. New York: Wiley, 1986.
[24] Ishiwata S, Hayashi M, Ohshima H, Suzuki O. J Soc Rheol Japan 1991;19:83.
[25] Hong PD, Huang HT. Polymer 2000;41:6195.
[26] Cotts PM, Selser JC. Macromolecules 1990;23:2050.
[27] Han CC, Ziya Akcasu A. Polymer 1981;22:1165.
[28] Ziya Akcasu A. Polymer 1981;22:1169.
[29] Nakamura Y, Inoue N, Norisuye T, Teramoto A. Macromolecules 1997;30:631.
[30] Kjoniksen AL, Nystrom B. Macromolecules 1996;29:7116.
[31] Burchard W, Schmidtn M, Stockmayer WH. Macromolecules 1980;13:580.
[32] Schmidt M, Burchard W. Macromolecules 1980;14:210.
[33] Herning T, Djabourov M, Leblond J, Takerkart G. Polymer 1991;32:3211.
[34] Bhatt M, Jamieson AM. Macromolecules 1988;21:3015.
[35] Fang L, Brown W. Macromolecules 1990;23:3284.
[36] Brown W, Fang L, Stepanek P. Macromolecules 1991;24:3201.
[37] Frisch HL, Simha R. In: Eirich FR, editor. Rheology, vol. 1. New York: Academic Press, 1956 (525pp.).
[38] Brown W. Macromolecules 1986;19:1083.
[39] Brown W, Zhou P. Macromolecules 1990;23:1131.
[40] Brown W, Johnsen P, Štepánek P, Jakeš J. Macromolecules 1988;21:2859.
[41] Brown W, Štepánek P. Macromolecules 1988;21:1791.
[42] Prcora R. Dynamic light scattering applications of photon correlation spectroscopy. New York: Plenum Press, 1985.
[43] Brown W, Fundin J. Macromolecules 1991;24:5171.
[44] Brown W. Dynamic light scattering: the method and some applications. Oxford: Clarendon Press, 1993.
[45] Brown W. Macromolecules 1984;19:66.
[46] Brown W, Fang L. Macromolecules 1990;23:3284.
[47] Pater P, Rodringuez F, Moloney G. J Appl Polym Sci 1979;23:2335.
[48] Robert MM, Jonathan MK. Tetrahedron Lett 1966:891.
[49] Symons MCR, Harvey JM, Jackson SE. J Chem Soc Farady Trans 1980;76:256.
[50] Sun THE, King J. Macromolecules 1996;29:3175.
[51] Guven O, Eltan E. Makromol Chem 1981;182:3129.
[52] Berry GC, Fox TG. Adv Polym Sci 1968;5:261.
[53] Raspaud E, Lairez D, Adam M. Macromolecules 1995;28:927.
[54] Adam MJ. Non-Crystal Solids 1991;131:773.
[55] Adam MJ, Delsanti M. J Phys (Paris) 1984;45:1513.
[56] Adam MJ, Delsanti M. J Phys (Paris) 1983;44:1185.